



Defence Research and
Development Canada

Recherche et développement
pour la défense Canada



MEMS-based light valves for ultra-high resolution projection displays

*F. Picard
INO, Sainte-Foy (Québec)*

*C. Campillo
INO, Sainte-Foy (Québec)*

*K.K. Niall
DRDC Toronto*

*C. Larouche
INO, Sainte-Foy (Québec)*

*H. Jerominek
INO, Sainte-Foy (Québec)*

DISTRIBUTION STATEMENT A
Approved for Public Release
Distribution Unlimited

Defence R&D Canada – Toronto
Technical Report
DRDC Toronto TR 2002-141
December 2002

Canada

20030331 049

MEMS-based light valves for ultra-high resolution projection displays

F. Picard
INO, Sainte-Foy (Québec)

C. Campillo
INO, Sainte-Foy (Québec)

K.K. Niall
DRDC Toronto

C. Larouche
INO, Sainte-Foy (Québec)

H. Jerominek
INO, Sainte-Foy (Québec)

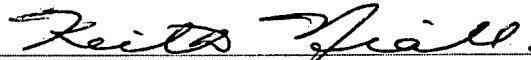
Defence R&D Canada - Toronto

Technical Report

DRDC Toronto TR 2002-141

December 2002

Authors



Keith K. Niall

Approved by



Lochlan Magee, PhD

Head, Simulation and Modelling for Acquisition, Rehearsal and Training Section

Approved for release by



K.M. Sutton

Chair, Document Review and Library Committee

Abstract

Ultra-high resolution projectors will improve the visual systems of military flight simulators dramatically. There are changes in aspect angle and aspect rate which fixed-wing fighter pilots can discriminate at long standoff distances, but which cannot be displayed with adequate resolution by the visual systems of contemporary flight simulators. At present the limit of display resolution is fixed by the capacity of the display's projector. This issue is being addressed by INO, DRDC, and their partners working toward the development of a new light-modulating micromirror MEMS (MicroElectroMechanical Systems). This unique device incorporates $25\text{ }\mu\text{m} \times 25\text{ }\mu\text{m}$ microbridges acting as flexible micromirrors. Each micromirror corresponds to one pixel of an image and is capable of modulating light intensity in analog fashion, with switching speeds in the range of $5\text{ }\mu\text{s}$. A linear array of micromirrors is combined with a scanning system, a microlaser light source and a Schlieren-type optical system to produce a 256 grey-level image. The result is a MOEMS (MicroOptoElectroMechanical Systems)-based system that can write thousands of image lines at a frame rate of 60 Hz.

Finite-element analyses have been performed to describe mechanical properties of the micromirrors. Several examples will be given from both static and dynamic electromechanical simulation. The micromirror fabrication process will be summarized. The physical characteristics of the micromirrors will be reported, including their response time and damage threshold. Finally, future plans will be described, including the development of 2000×1 linear pixel arrays with the associated control electronics.

Résumé

Les projecteurs à très haute résolution devraient permettre d'améliorer considérablement les systèmes visuels des simulateurs de vol militaires. Des variations dans la précision de l'angle de présentation et des changements dans cet angle de présentation qui sont distinguées à grande distance par les pilotes des avions de chasse ne sont actuellement pas affichées avec la résolution adéquate par les systèmes de visualisation des simulateurs. Leur résolution est, pour l'instant, limitée par la capacité du projecteur d'affichage. Le sujet est étudiée par l'INO et ses partenaires qui travaillent à l'élaboration d'un nouveau modulateur de lumière incluant des micromiroirs de type MEMS (microsystème électromécanique). Ce dispositif unique est composé de microponts de $25\text{ }\mu\text{m} \times 25\text{ }\mu\text{m}$ qui agissent comme des micromiroirs souples. Chaque micromiroir correspond à un pixel image et permet de moduler l'intensité lumineuse de manière analogique, avec des vitesses de commutation de l'ordre de $5\text{ }\mu\text{s}$. Un réseau linéaire de micromiroirs est conjugué à un système de balayage, à une source lumineuse microlaser et à un système optique de type Schlieren en vue de produire une image à 256 niveaux de gris. Il en résulte un système basé sur des éléments MOEMS (microsystème opto-électromécanique) capable d'afficher des milliers de lignes à une fréquence d'images de 60 Hz.

Des analyses par éléments finis ont été réalisées dans le but de décrire les propriétés mécaniques des micromiroirs. Plusieurs exemples de simulations électromécaniques en mode statique et en mode dynamique seront présentés. Le processus de fabrication des micromiroirs sera résumé. Les caractéristiques physiques des micromiroirs, incluant leur temps de réponse et leur seuil de dommage seront indiquées. Enfin, les travaux futurs comprenant l'élaboration de réseaux de 2000×1 pixels linéaires associés à leur électronique de commande seront décrits.

This page intentionally left blank.

Executive summary

Until now, the resolution of visual displays has limited the usefulness of military flight simulators for training fighter maneuvers in fast fixed-wing aircraft. One means to resolve this deficiency has been to develop visual projection systems with unprecedented resolution. One promising approach is based on optical systems which have solid state lasers as their light source and a MEMS (MicroElectroMechanical Systems) device as their light modulator or light valve. This light valve consists of a linear array of microbridges which act as flexible micromirrors. The micromirrors move electrostatically in response to applied voltage. The present report is a summary of results on the simulation, fabrication, and characterization of the light valve. 510×1 micromirror arrays have been fabricated using surface micromachining techniques. The starting material is a silicon wafer on which a silicon nitride film has been deposited. An aluminum layer is deposited and patterned to produce a bottom electrode. The micromirror fabrication starts with definition of a platform in a relatively thick sacrificial polyimide layer. Next is the deposition and patterning of an aluminum alloy thin film. Finally the sacrificial polyimide layer is etched, creating an air gap between membrane and substrate. Three main features of the light valve's performance have been characterized: static response to voltage, dynamic response, and damage threshold. It was found that membrane oscillation can be reduced significantly by selecting the time constant of an exponentially varying driving voltage. The time required to stabilize the micromirror can be as short as 2.6 μsec . Micromirror width does not have an important effect on static membrane performance. However, when dynamic response is considered the situation changes significantly. Thermal and stress analyses have been simulated to estimate damage thresholds for $25 \times 25 \mu\text{m}$ micromirrors. At the same time, an optical method has been used to characterize the dynamic response of fabricated micromirrors. No visible damage was shown for incident laser intensities up to 8000 W/cm^2 . These experimental results are in good agreement with simulation estimates of 8850 W/cm^2 . The micromirror damage threshold is not limited by the melting temperature of the aluminum alloy, but by its mechanical yield. The characteristics of these flexible micromirrors make the present light valve an appropriate modulator for the new generation of ultra-high resolution projectors. A fully-addressable 2000-element micromirror array is currently under development.

Picard, F., Campillo, C., Niall, K.K., Larouche, C., Jerominek, H. (2002). MEMS-based light valves for ultra-high resolution projection displays. DRDC Toronto TR 2002 - 141. Defence R&D Canada - Toronto.

Sommaire

Jusqu'à présent, la résolution des affichages visuels limitait l'efficacité des simulateurs de vol militaires dans les manœuvres de formation sur les avions de combat rapides à voilure fixe. L'une des façons de combler cette lacune a été d'élaborer des systèmes de projection visuels avec une résolution sans précédent. Une des démarches prometteuses est basée sur les systèmes optiques qui comportent des lasers à semiconducteurs comme source lumineuse et un dispositif MEMS (microsystème électromécanique) comme modulateur de lumière. Ce modulateur de lumière est constitué d'un réseau linéaire de microponts qui agissent comme des micromiroirs souples. Les micromiroirs se déplacent électrostatiquement en réponse à une tension appliquée. Le présent rapport comprend un résumé des résultats obtenus après la simulation, la fabrication et la caractérisation du modulateur de lumière. Des réseaux de micromiroirs de 510×1 sont fabriqués à l'aide des techniques de micro-usinage de surface. Le matériau de départ est une plaquette de silicium sur laquelle une couche de nitrure de silicium a été déposée. Une couche d'aluminium est ensuite déposée et définie de manière à produire une électrode. La fabrication du micromiroir débute avec la définition d'une plateforme dans une couche de polyimide sacrificielle relativement épaisse. Ensuite, on procède au dépôt et à la définition d'une couche mince en alliage d'aluminium. Enfin, la couche de polyimide sacrificielle est gravée, ce qui crée une couche d'air entre la membrane et le substrat. Trois des grandes caractéristiques de la performance du modulateur de lumière ont été caractérisées, il s'agit de la réponse statique à la tension, de la réponse dynamique et du seuil de dommage. On a découvert que l'oscillation de la membrane peut être considérablement réduite en choisissant la constante de temps pour une tension de commande qui varie exponentiellement. Le temps requis pour stabiliser le micromiroir peut être aussi court que $2,6 \mu\text{s}$. La largeur du micromiroir n'a pas, à priori, une incidence importante sur la performance statique de la membrane. Cependant, lorsque l'on considère la réponse dynamique, la situation est très différente. De plus, une méthode optique a été employée pour caractériser la réponse dynamique des micromiroirs fabriqués. Les analyses des caractéristiques thermiques et des contraintes ont été simulées pour estimer les seuils de dommage pour des micromiroirs de $25 \times 25 \mu\text{m}$. Aucun dommage visible n'a été signalé pour une intensité du laser incident allant jusqu'à $8\,000 \text{ W/cm}^2$. Ces résultats expérimentaux sont conformes aux estimations de la simulation de 8850 W/cm^2 . Les dommages causés au micromiroir ne sont pas limités par la température de fusion de l'alliage d'aluminium, mais par son rendement mécanique. Les caractéristiques de ces micromiroirs souples font de ce modulateur de lumière un modulateur approprié pour la nouvelle génération de projecteurs à résolution ultra élevée. Un réseau de micromiroirs à 2000 éléments entièrement contrôlable est actuellement en cours d'élaboration.

Picard, F., Campillo, C., Niall, K.K., Larouche, C., Jerominek, H. (2002). MEMS-based light valves for ultra-high resolution projection displays. DRDC Toronto TR 2002 - 141. Defence R&D Canada - Toronto.

Table of contents

Abstract	i
Résumé	i
Executive summary	iii
Sommaire	iv
Table of contents	v
List of figures	vi
List of tables	vii
Acknowledgments	viii
Introduction	1
Micromirror performance simulation	3
Electromechanical static simulations	3
Dynamic simulations	5
Thermal simulations	8
Micromirror fabrication	9
Fabrication process flow	9
Fabrication results	11
Micromirror characterization	13
Micromirror static response	14
Micromirror dynamic response	15
Micromirror damage threshold	16
Future direction	17
References	18

List of figures

Figure 1. Light modulation approach with flexible micromirrors.....	1
Figure 2. Flexible micromirror structure (W: mirror width, L: mirror length, G: mirror/substrate gap size, t: membrane thickness)	3
Figure 3. Simulation of the micromirror static response for a membrane thickness of 0.1 μm . Structure dimensions: L: 25 μm , W: 25 μm , t: 0.1 μm , G: 2.5 to 4.5 μm	4
Figure 4. Simulation of the micromirror static response for a membrane thickness of 0.15 μm . Structure dimensions: L: 25 μm , W: 25 μm , t: 0.15 μm , G: 2.5 to 4.5 μm	4
Figure 5. Simulation of the micromirror static response for L: 15 μm and W: 25 μm	5
Figure 6. Simulation of the micromirror dynamic response to a 158 V step function. Structure dimensions: L: 25 μm , W: 25 μm , t: 0.15 μm , G: 4.5 μm	6
Figure 7. Simulation of the micromirror dynamic response to an exponential voltage variation with a time constant of 0.43 μs . Structure dimensions: L: 25 μm , W: 25 μm , t: 0.15 μm , G: 3 and 4.5 μm	6
Figure 8. Simulation of the micromirror dynamic response to an exponential voltage variation with a time constant of 0.43 μs . Structure dimensions: L: 25 μm and W: 25 μm	7
Figure 9. Simulation of the micromirror dynamic response to exponential voltage variations. Structure dimensions: L: 15 μm , W: 25 μm , t: 0.1 μm , G: 2 μm	7
Figure 10. Simulation of the micromirror dynamic response for decreasing exponential voltage variations and a decreasing pressure ramp. Structure dimensions: L: 25 μm , W: 25 μm , t: 0.15 μm , G: 4.5 μm	8
Figure 11. Simulation of the mirror dynamic response for a decreasing pressure ramp of 2 μs for 2 different mirror widths. Structure dimensions: L: 25 μm , t: 0.15 μm , G: 4.5 μm	8
Figure 12. Flexible micromirror fabrication process flow	10
Figure 13. Flexible micromirrors (Nominal dimensions are L: 30 μm , W: 25 μm , t: 0.15 μm , G: 4.7 μm , spacing between mirrors: 2 μm)	11
Figure 14. Flexible micromirrors (Nominal dimensions are L: 20 μm , W: 25 μm , t: 0.15 μm , G: 4.7 μm , spacing between mirrors: 3 μm)	11
Figure 16. Set-up for the micromirror dynamic response characterization.....	13
Figure 17. Static response of a micromirror with compressive residual stress (Nominal micromirror dimensions are L: 25 μm , W: 25 μm , t: 0.15 μm , G: 4.7 μm)	14

Figure 19. Dynamic response of a micromirror with compressive residual stress (Nominal micromirror dimensions are L: 25 μm , W: 25 μm , t: 0.15 μm , G: 4.7 μm)15

Figure 20. Dynamic response of a micromirror with tensile residual stress (Nominal micromirror dimensions are L: 25 μm , W: 25 μm , t: 0.15 μm , G: 4.7 μm)16

List of tables

Table 1- Fabrication parameters.....9

Acknowledgments

We would like to thank Brian Welch and Andrew Fernie of CAE Inc. for their contribution and support. Marty Schenker designed the initial optical system. The thermal simulations are due to Nichola Desnoyers of INO. This work was supported by Defence Research & Development Canada, under PWGSC contracts W7711-007650 and W7711-017736.

Introduction

The resolution of contemporary visual displays imposes limits on the usefulness of military flight simulators in training. At medium standoff distances in air-to-air engagements, there are too many features that pilots can discern by eye but which cannot yet be properly represented on a visual display. Judgments that are part of basic fighter manoeuvres (of angle off, aspect angle, and aspect rate) are still better made by the eye at long ranges in the air than in a simulator. Currently, the approach to handling these situations is to add small field of view (FOV), high resolution projectors specifically for air targets. There are, however, inherent limitations in this approach in terms of the number of targets that can be represented at high resolution as well as in the contrast of the target relative to the background image. Providing the required resolution performance without the limitations of target projectors requires the development of new projection systems with unprecedented resolution. The performance of these projectors should be such that 20 megapixel images can be displayed at a frame rate of 60 Hz. A promising approach to reach the required performance is based on optical systems comprising a solid state laser as the light source and MicroElectroMechanical System (MEMS) devices as the light modulators. One such optical system including a new MEMS device has been developed by INO and its partners. The active element of this projector is a linear array of microbridges acting as flexible micromirrors. This mirror array is illuminated with a laser source and produces an image line at the output of an optical relay. Each pixel of the image line corresponds to one flexible micromirror which modulates the pixel intensity in an analog fashion with switching times in the range of 5 μ s. The light modulating scheme (see Figure 1) employs Schlieren optics [1] which translate the micromirror curvature into light intensity at the Schlieren relay output.

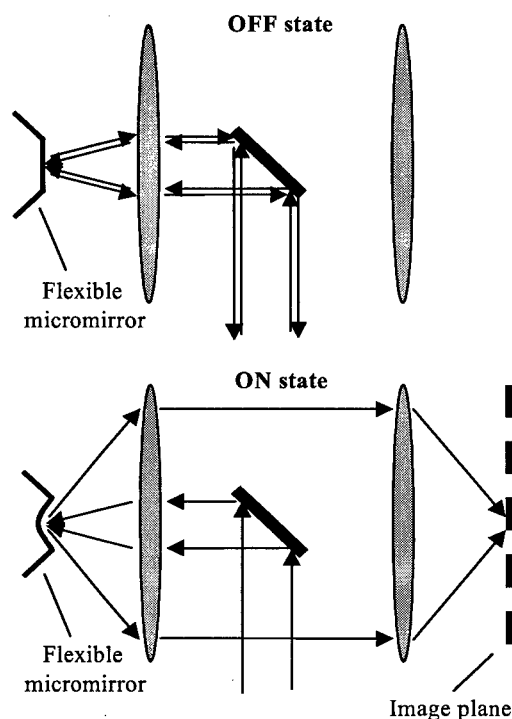


Figure 1. Light modulation approach with flexible micromirrors

The projector design assumes a maximum micromirror curvature corresponding to a f-number of two. The maximum mirror sag or deflection is obtained, in parabolic approximation, using the following expression:

$$\delta_{\max} = L / 32 \quad (1)$$

where L is mirror length. Micromirror curvature is controlled by electrostatic actuation. A complete 2-D image is obtained by a scanning mechanism that displays each image column sequentially. Projection optics are used to tailor the final image.

One crucial component of this projection system is the flexible micromirror which is the basic building block of the MEMS modulator array. In the following, results will be reported from the simulation, fabrication and characterization of the micromirrors.

Micromirror performance simulation

Electromechanical static simulations and dynamic simulations were performed to establish the basic micromirror design. The MEMS simulation software Intellisuite™ was used for these simulations. Thermal simulations with the software ANSYS™ have been performed to estimate the micromirror damage threshold. The simulated micromirror structure (see Figure 2) consists of a reflecting area whose curvature can be modified, two legs supporting the mirror a few microns above the substrate and an electrode on the substrate underneath the mirror. For the purpose of the simulation, the micromirror material was assumed to be aluminum with a low residual tensile stress of 10 MPa.

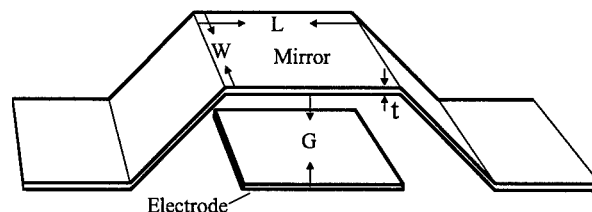


Figure 2. Flexible micromirror structure (*W*: mirror width, *L*: mirror length, *G*: mirror/substrate gap size, *t*: membrane thickness)

When a voltage is applied between mirror and electrode, an electrostatic force is generated which curves the mirror toward the substrate. As voltage is increased, mirror curvature increases. At some point, the restoring force caused by the membrane curvature cannot counterbalance the electrostatic force; the mirror either stops as it touches the substrate or it collapses. This phenomenon is called "pull-in" instability; it is caused by nonlinear variation of electrostatic force with mirror curvature. This is the primary factor limiting the analog control range for the micromirror curvature.

Electromechanical static simulations

Electromechanical static simulations have been performed to estimate required micromirror dimensions. The structure must exhibit control range sufficient to reach the mirror curvature required for the projector system. This must be achieved with an activation voltage as low as possible. In addition, the structure fabrication must remain feasible.

The simulations explored the influence of the following parameters: membrane length (*L*), membrane width (*W*), membrane thickness (*t*) and gap size between the membrane and the underlying electrode (*G*) (see Figure 2 for definitions). Structures exhibiting a membrane thickness of 0.1 μm or more had to be considered to keep the structure both manufacturable and rugged. Gap size had to be a few micrometers only (1.5 to 4.5 μm typically) to maintain a reasonably low maximum activation voltage. This caused structures with a membrane length of 30 μm or more to exhibit a maximum activation voltage very close to the pull-in threshold. For this reason, the study considered mainly membrane lengths shorter than 30 μm . Membrane width was not found to have a significant impact on static performance.

The most relevant simulation results (see Figures 3, 4 and 5) were obtained for structures with a membrane width of 25 μm . Similar results were obtained for 10 μm wide membranes. For 25 μm x 25 μm membranes, the simulations indicate that (see Figures 3 and 4) the minimum gap size between mirror and substrate is 3.5 μm for a 0.1 μm thick membrane and around 3 μm for a 0.15 μm membrane. This corresponds to maximum activation voltages of 76 V and 120 V for membrane thicknesses of 0.1 and 0.15 μm , respectively. For smaller gap sizes, the micromirrors are very close to or beyond the pull-in threshold at maximum deflection.

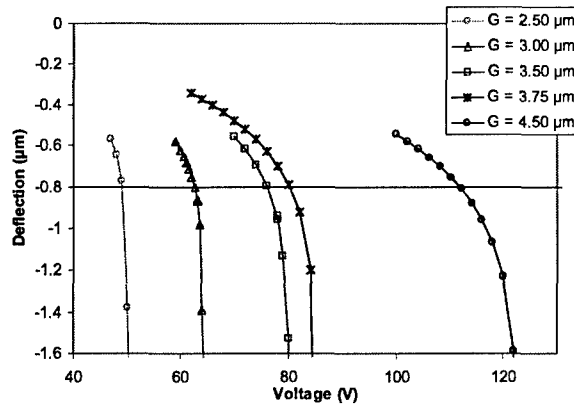


Figure 3. Simulation of the micromirror static response for a membrane thickness of 0.1 μm . Structure dimensions: L: 25 μm , W: 25 μm , t: 0.1 μm , G: 2.5 to 4.5 μm

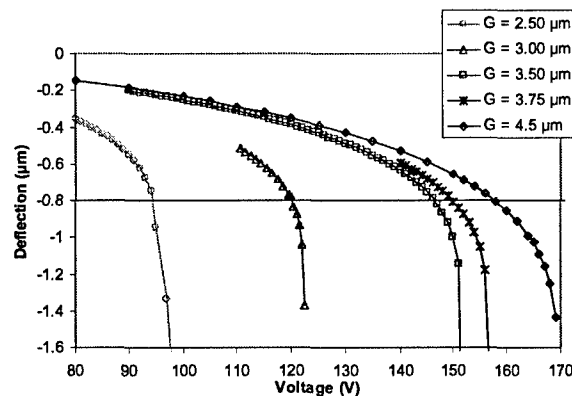


Figure 4. Simulation of the micromirror static response for a membrane thickness of 0.15 μm . Structure dimensions: L: 25 μm , W: 25 μm , t: 0.15 μm , G: 2.5 to 4.5 μm

When the membrane length is reduced to 15 μm , the required maximum deflection decreases. This allows a reduction of the gap size (see Figure 5) to 2 μm for 0.1 or 0.15 μm thick membranes without reaching the pull-in threshold at maximum deflection. As the micromirror structure is shortened, it becomes stiffer

and activation voltage increases to 95 V and 165 V for membrane thicknesses of 0.1 and 0.15 μm , respectively.

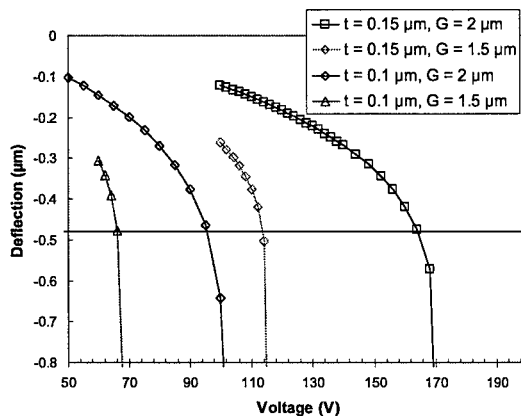


Figure 5. Simulation of the micromirror static response for L : 15 μm and W : 25 μm

Experimental testing on unpassivated test structures determined that limiting the electrical field to 70 $\text{V}/\mu\text{m}$ is a good design rule to avoid arcing. Electrostatic discharge could occur when a 0.15 μm thick membrane is fully deflected since the maximum electric field is then 110 $\text{V}/\mu\text{m}$. The best simulated 15 μm long membrane is the one with a thickness of 0.1 μm . The main advantage of this structure is that it can have shorter response times than the 25 μm x 25 μm micromembranes.

Dynamic simulations

The model used for the dynamic simulations included structural and squeeze film damping effects [2]. The electrostatic pressure field acting on the membrane and varying with the mirror deflection had to be converted into a uniform pressure field varying with time but which was not linked directly with mirror curvature. This conversion was necessary for the MEMS simulation software and is considered an acceptable simplification for estimating dynamic performance of the microdevice. Uniform pressure had to stabilize at a value corresponding to the required micromirror deflection. The dynamic simulations studied different pressure variations with time. Pressure variations corresponding to a voltage step function or to an exponentially varying voltage are of particular interest since their implementation is relatively straightforward. The correspondence between voltage and pressure is obtained by determining what uniform pressure would produce the same static deflection as a given voltage. For the dynamic study, the time required by the micromirror to oscillate within $\pm 5\%$ of the maximum deflection value was used as a figure of merit to evaluate a given structure activated with a given pressure variation in time.

The response of a membrane (25 μm x 25 μm , 0.15 μm thick, suspended 4.5 μm above the substrate) to a pressure step function (see Figure 6) shows that this system is clearly underdamped. This causes the membrane to overshoot and oscillate around its equilibrium position for a relatively long time.

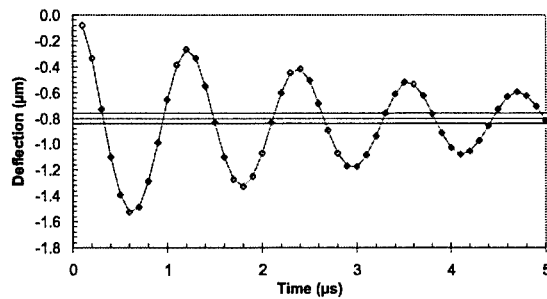


Figure 6. Simulation of the micromirror dynamic response to a 158 V step function. Structure dimensions: L : 25 μm , W : 25 μm , t : 0.15 μm , G : 4.5 μm

Since the membrane stabilization time is a critical parameter for projection applications, simulations using other pressure vs time functions have been performed to minimize the oscillations of the mirror. Uniform pressures corresponding to an exponentially varying voltage have been investigated. Results for the same structure as Figure 6 are presented together with results for the 25 μm x 25 μm membrane structures from the static study (see Figures 7 and 8). These results indicate it is possible to reduce membrane oscillation significantly by selecting the time constant of the exponential function carefully. For the structures considered, a time constant of 0.43 μs achieved settling times typically shorter than 5 μs and even times below 2 μs . Similar results are presented for the 15 μm long structure selected from the static study (see Figure 9). There the settling time is about 2 μs for a time constant of 0.43 μs and shorter than 1 μs for a time constant of 0.22 μs .

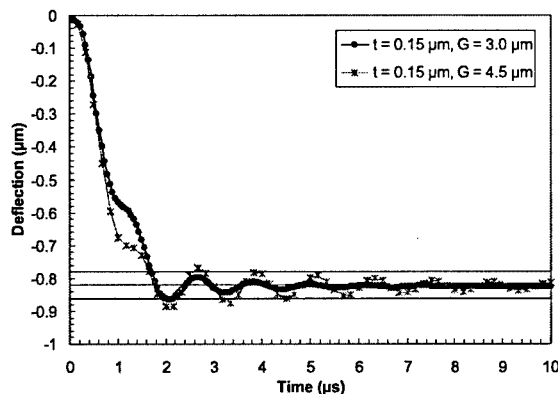


Figure 7. Simulation of the micromirror dynamic response to an exponential voltage variation with a time constant of 0.43 μs . Structure dimensions: L : 25 μm , W : 25 μm , t : 0.15 μm , G : 3 and 4.5 μm

All these dynamic results were obtained for a mirror deflection varying from 0 μm to the maximum deflection required to achieve a mirror f -number of two. When the inverse case is considered (from maximum deflection to zero), it becomes more difficult to reduce mirror oscillations using pressure variations corresponding to an exponentially decreasing voltage since pressure is a nonlinear function of applied voltage. For the structure of Figure 6 with a voltage decreasing exponentially the settling time is

about 9 μs . If the time constant is increased to 3.26 μs , the settling time decreases to 5.3 μs which is similar to the settling time from 0 to maximum deflection (4.6 μs with a time constant of 0.43 μs). Results for a decreasing pressure ramp going to zero after 2 μs are also presented. These indicate that this type of pressure variation is effective in reducing the membrane oscillations. The time required to stabilize the membrane is as short as 2.6 μs .

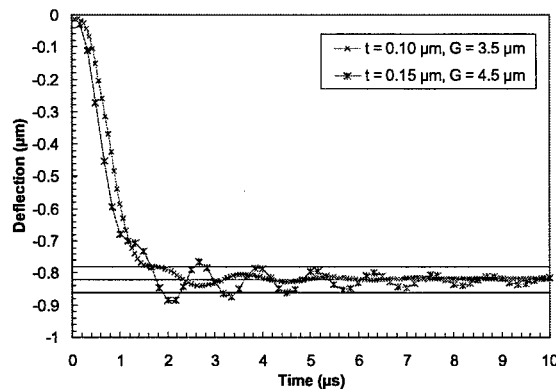


Figure 8. Simulation of the micromirror dynamic response to an exponential voltage variation with a time constant of 0.43 μs . Structure dimensions: L : 25 μm and W : 25 μm

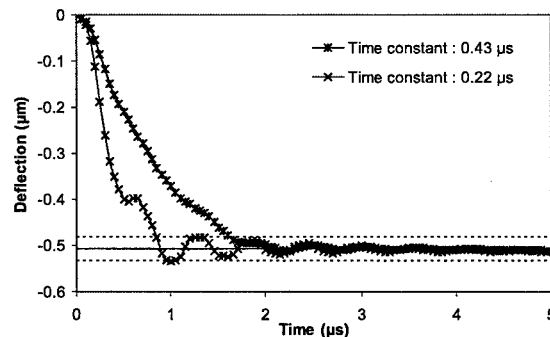


Figure 9. Simulation of the micromirror dynamic response to exponential voltage variations. Structure dimensions: L : 15 μm , W : 25 μm , t : 0.1 μm , G : 2 μm

Micromirror width does not have an important effect on static membrane performance. However, when dynamic response is considered, the situation changes significantly. This is illustrated by comparing the response of a 10 μm wide membrane with the response of a 25 μm membrane. All other membrane dimensions are unchanged. The uniform pressure applied in both cases is ramped and decreases to zero after 2 μs . Settling time increases from 2.6 to 9 μs when membrane width is decreased from 25 to 10 μm (see Figure 11). This demonstrates that squeeze film damping reduction is important for a 10 μm wide membrane. The 10 μm wide membrane settling time could be reduced by increasing pressure ramp duration above 2 μs . However, this approach would not allow a match to the 25 μm membrane performance.

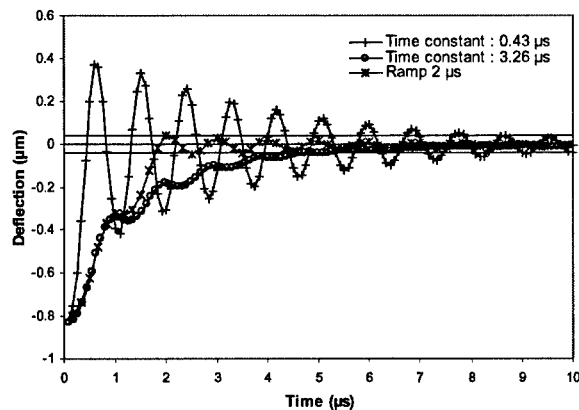


Figure 10. Simulation of the micromirror dynamic response for decreasing exponential voltage variations and a decreasing pressure ramp. Structure dimensions: L : 25 μm , W : 25 μm , t : 0.15 μm , G : 4.5 μm

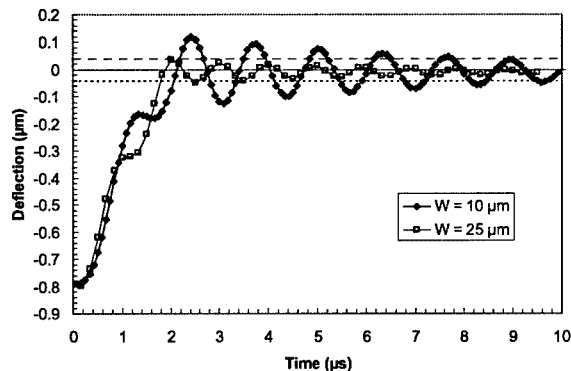


Figure 11. Simulation of the mirror dynamic response for a decreasing pressure ramp of 2 μs for 2 different mirror widths. Structure dimensions: L : 25 μm , t : 0.15 μm , G : 4.5 μm

Thermal simulations

Thermal and stress analyses have been performed with ANSYSTM software to estimate the damage threshold for 25 x 25 μm micromembranes. These simulations indicate that a membrane initially at 20°C could absorb up to 6750 W/cm² before reaching 450°C that is about 75 % of the melting point of the Al alloy. Assuming optical absorption of 10 % for the alloy, this means that an optical power density of 67.5 kW/cm² could illuminate the membrane before its temperature reached 450 °C. However, stress analysis revealed that the Al alloy yield – about 190 MPa – is reached in some points when absorbed power density is 885 W/cm². Membrane damage threshold is then estimated to correspond to an incident optical power density of about 8850 W/cm². Most importantly, the damage threshold for the studied micromirror structure is not limited by the Al alloy melting temperature but by the Al alloy mechanical yield.

Micromirror fabrication

510 x 1 micromirror arrays have been fabricated using surface micromachining techniques [3]. The micromirror design is based on general rules that emerge from the simulations and from the fabrication process. However, the material properties and residual stress were not perfectly known for the simulation. To take into account possible differences between the simulated and measured mirror characteristics, microdevices exhibiting dimensions varying slightly about those selected from the simulations have been produced. Nevertheless each fabricated array comprised only one mirror design. Table I summarizes the parameters used for the fabrication. All possible combinations of membrane dimensions for a given gap size were fabricated simultaneously on one silicon wafer. The gap size was the same for all structures on a given wafer but was varied from wafer to wafer.

Table 1- Fabrication parameters

Mirror parameter	Dimension (μm)
Mirror length	20, 25 and 30
Mirror width	10 and 25
Gap size	3.5 and 4.5
Distance between mirrors	2, 3 and 5

Fabrication process flow

The fabrication process uses just four or even three photolithographic steps. The starting material is a silicon wafer on which a silicon nitride (SiN) film has been deposited for electrical isolation. A first metallic layer is deposited and patterned to produce the bottom electrode (see Figure 12). This metallic layer material can be aluminum or gold. The electrode is passivated using a SiN layer and windows are opened in the SiN to provide bonding pads. This passivation step is optional: it is not required to achieve functional micromembranes. The membrane fabrication starts with the definition of a platform in a relatively thick sacrificial polyimide layer. The next step is the deposition and patterning of an aluminum alloy thin film. The aluminum alloy layer is deposited using Physical Vapor Deposition (PVD). This aluminum alloy film is patterned using a photoresist mask and wet etching. This produces the micromembrane itself. Finally, the sacrificial polyimide layer is isotropically etched using a plasma asher which generates an air gap between membrane and substrate.

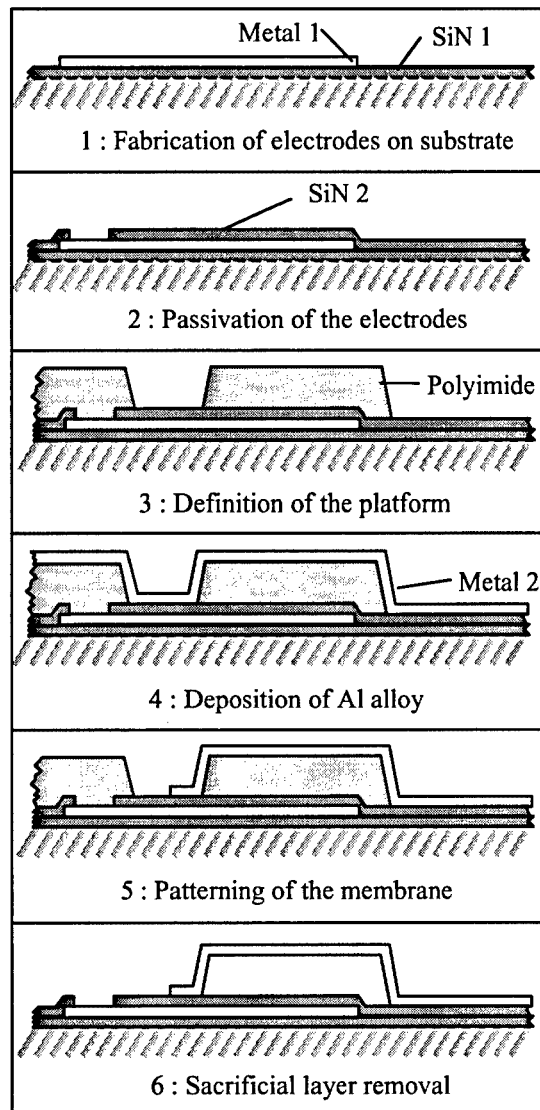


Figure 12. Flexible micromirror fabrication process flow

Fabrication results

The process described above has been used to fabricate the micromirror arrays. The structures exhibit a smooth reflecting surface and are relatively flat (see Figures 13, 14 and 15). At the mirror level, typical structures show a membrane width narrower than the nominal width. Moreover, the legs supporting the mirror are slightly wider on the substrate than at the mirror level. The photoresist used to mask the Al alloy for the etching step does not cover the wafer topography conformally. This results in a photoresist mask which does not match the photomask pattern perfectly. This difference and some undercut during the Al alloy wet etching cause geometrical imperfections.

The texture on the leg surface is the reproduction of the surface relief of sacrificial polyimide which supported the leg before being removed. This texture is typical of polyimide walls obtained by dry etching. Finally, small defects can be observed at the membrane edges (see Figure 14). Characterizations performed on the membranes indicate that these defects do not distort the mirror profile significantly.

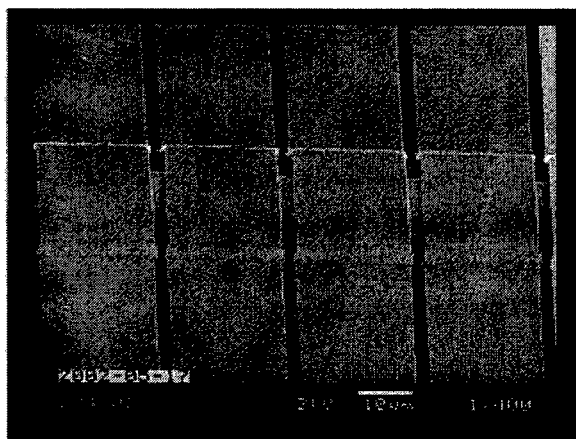


Figure 13. Flexible micromirrors (Nominal dimensions are L: 30 μm , W: 25 μm , t: 0.15 μm , G: 4.7 μm , spacing between mirrors: 2 μm)

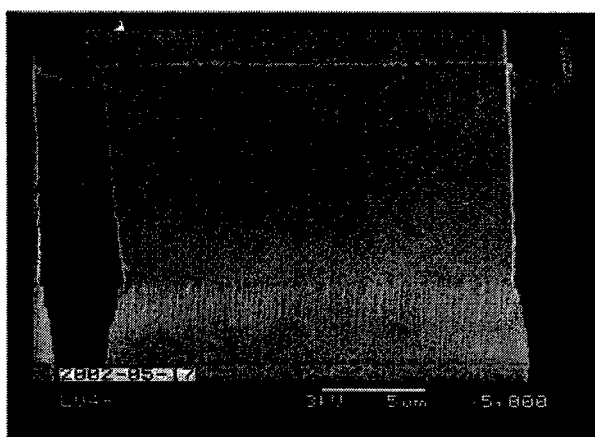


Figure 14. Flexible micromirrors (Nominal dimensions are L: 20 μm , W: 25 μm , t: 0.15 μm , G: 4.7 μm , spacing between mirrors: 3 μm)

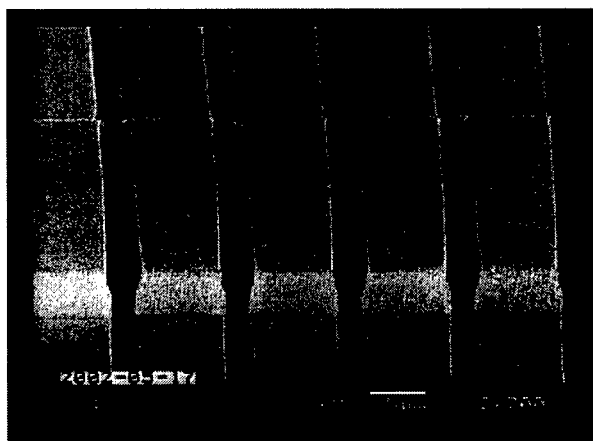


Figure 15. Flexible micromirrors (Nominal dimensions are L: 25 μm , W: 10 μm , t: 0.15 μm , G: 4.7 μm , Spacing between mirrors: 2 μm)

Micromirror characterization

Three main aspects of the micromirror performance have been characterized: static response, dynamic response and damage threshold. The static response was characterized by measuring the mirror deflection as a function of the voltage applied between the membrane and the underlying electrode. The membrane deflection was measured using a microscope equipped with a 10 x Mireau interference objective with a numerical aperture of 0.25. The wavelength of the light illuminating the mirror under test was 548 nm. This produced an interference pattern in which two consecutive dark or light fringes were generated by mirror regions separated by a vertical distance of 0.27 μm . The voltage was applied gradually across the MEMS light valve. The corresponding mirror deflection was measured by recording the fringe number between the mirror center and the mirror edges.

An optical method (see Figure 16) has been used to characterize the dynamic response of the micromirror. The micromirror under test is illuminated with a laser beam and the reflected diffraction pattern is observed through a microscope. When the micromirror curvature is changed, the observed diffraction pattern is modified and some regions of the intensity profile show an important intensity variation. A photodetector is positioned at the microscope output to measure the intensity corresponding to these high contrast regions. The photodetector response time was short enough (about 10 ns) to provide time resolved intensity measurements. The voltage waveform applied to the micromembrane and the photodetector signal are recorded simultaneously using an oscilloscope. The measured signals allowed characterization of the micromirror dynamic response.

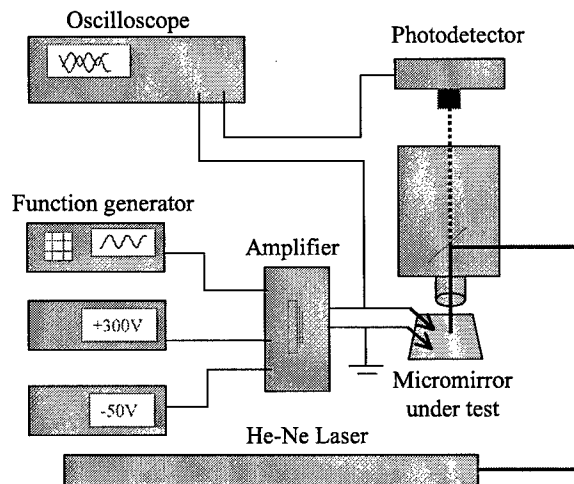


Figure 16. Set-up for the micromirror dynamic response characterization

Finally, a doubled YAG laser source was focussed on groups of micromirrors to evaluate damage threshold. The micromembranes were illuminated with a fixed laser intensity. After each illumination session of a few minutes, the micromirrors were examined with a microscope to verify if visible damage

had occurred. Laser intensity was then increased and the procedure repeated until the mirrors were damaged.

Micromirror static response

Micromirror curvature for an applied voltage of 0 V depends on residual stress in the membrane. Compressive residual stress causes a convex initial curvature while tensile residual stress results in a downward membrane deflection. Micromirrors exhibiting different residual stresses and initial curvatures have been fabricated by varying Examples of the static response for micromirrors (see Figures 17 and 18) exhibiting residual compressive and tensile stresses are presented. For a membrane with compressive stress, a voltage can be applied to return mirror curvature to a minimum value corresponding to a deflection of 0 μm . In the example (see Figure 17), this offset voltage is about 136 V and a deflection of 0.8 μm corresponding to a f-number of two is reached with 233 V. The membrane with a tensile residual stress (see Figure 18) exhibits a downward deflection at 0 V. In the example, this deflection is 0.25 μm which represents a significant part of the required analog deflection range. A deflection of 0.8 μm corresponding to a f-number of 2 is achieved with 158 V.

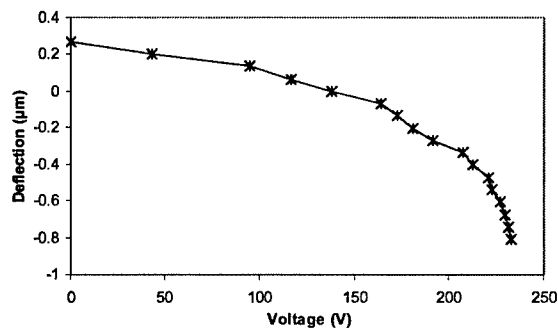


Figure 17. Static response of a micromirror with compressive residual stress (Nominal micromirror dimensions are L: 25 μm , W: 25 μm , t: 0.15 μm , G: 4.7 μm)

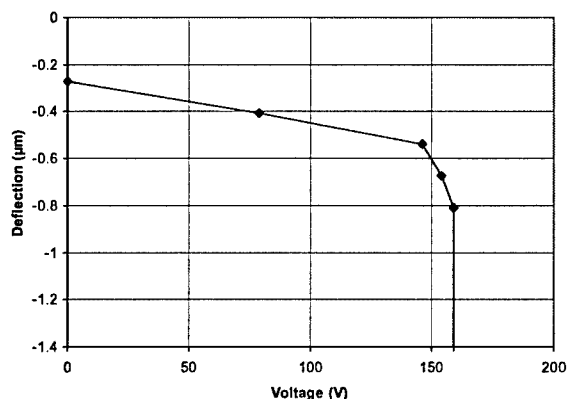


Figure 18. Static response of a micromirror with tensile residual stress (Nominal micromirror dimensions are L: 25 μm , W: 25 μm , t: 0.15 μm , G: 4.7 μm)

It is clear that a membrane with a tensile residual stress has the advantage of reaching maximum deflection at a lower voltage than a membrane with compressive residual stress. Moreover, the available deflection range is covered with a larger voltage span which reduces the voltage resolution requirement. Membranes with a residual tensile stress also have major drawbacks. First, the available analog deflection range is reduced. Second, the deflection state corresponding to the projector black level cannot be adjusted with a voltage offset. This can have an important impact on projector contrast. Although it typically requires a higher activation voltage and a better voltage resolution, a membrane with compressive residual stress is a good trade-off for projection since contrast is key to these applications.

Micromirror dynamic response

The dynamic response of micromirrors exhibiting either compressive or tensile residual stress is presented. For these examples, membranes are moved from minimum to maximum deflection, then back to the minimum deflection. The voltage waveforms used to control the membranes are also shown. For compressive residual stress (see Figure 19), the activation voltage waveform is added to the voltage offset required to achieve a membrane deflection of 0 μm . The applied voltage waveform transient time is a little less than 2 μs . When the membrane is activated, it stabilizes in about 10 μs . With this voltage waveform, the stabilization time is even longer when the micromembrane is deactivated. These relatively long settling times combined with the important membrane oscillations about the equilibrium position indicate that this voltage waveform is not adapted to activation of the micromirror under test. The voltage variation rate is too high; it should be reduced by increasing the transient time to 3 or 4 μs .

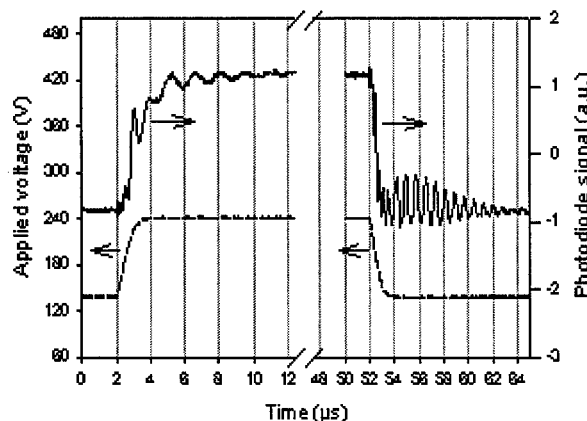


Figure 19. Dynamic response of a micromirror with compressive residual stress (Nominal micromirror dimensions are L : 25 μm , W : 25 μm , t : 0.15 μm , G : 4.7 μm)

In the case of a membrane with a tensile residual stress (see Figure 20), no voltage offset is applied to the membrane under test. A waveform with a transient time of 3 μs has been used to control the micromirror. When activated, the micromembrane stabilizes in 4 μs and the settling time required to bring it back to its minimum deflection position is less than 5 μs .

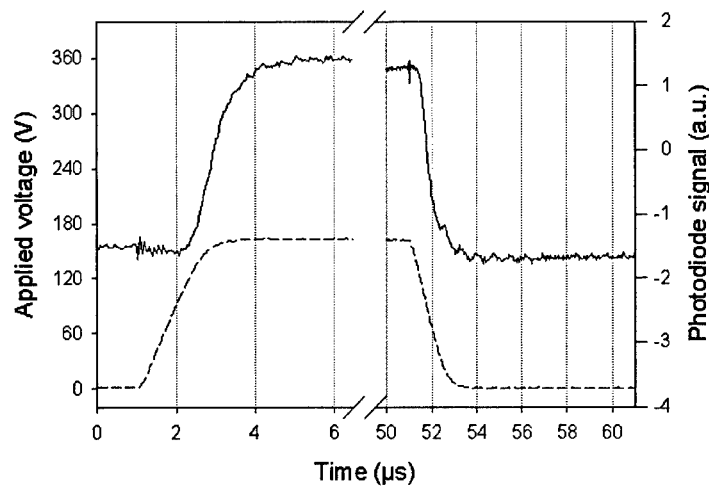


Figure 20. Dynamic response of a micromirror with tensile residual stress (Nominal micromirror dimensions are L : 25 μm , W : 25 μm , t : 0.15 μm , G : 4.7 μm)

Micromirror damage threshold

The test performed to determine the membrane damage threshold showed no visible damage for incident laser intensities up to 8000 W/cm². However, permanent membrane deformations are observed for a laser intensity of 16000 W/cm². These experimental results are in good agreement with simulation estimates of 8850 W/cm². The simulations also predicted that thermally generated stresses exceeding the material yield would cause device failure.

Future direction

The characteristics of the described flexible micromirror make it an appropriate light modulator for ultra-high resolution microlaser projectors. This new class of devices finds its application in displays for military flight simulation, specifically in simulators for fast jets (not to mention their commercial applications in digital cinema). A fully addressable 2000-element micromirror array is currently under development. A standard high-voltage CMOS process will be used to fabricate the custom integrated circuit required to control this linear array. Challenging issues related to the packaging of these large arrays are being addressed. New geometries for flexible micromirrors are also being considered. The aims of this design review are to decrease the micromirror activation voltage and settling time. Moreover, flexible micromirror arrays have been integrated into a prototype projector. This projection system provides a test bench to optimize the system configuration and its components. Globally, technological advances have already been made or are ongoing on several fronts in the development of this MEMS-based projector. When combined into a unique system, these advances are expected to result in a high performance projector with a resolution of 20 megapixels operating at a frame rate of 60 Hz.

References

1. Van Raalte, J. A. (1970). A new Schlieren light valve for television projection. *Applied Optics*, 20, 2225-2230.
2. Yang, Y.-J., & Senturia, S. D. (1996). Numerical simulation of compressible squeezed-film damping. In *Technical Digest of the Solid State Sensor and Actuator Workshop*. Hilton Head Island, SC: Transducer Research Foundation, Inc., pp. 76 – 80.
3. Madou, M. (1997). *Fundamentals of microfabrication*. Boca Raton: CRC Press.

DOCUMENT CONTROL DATA SHEET

1a. PERFORMING AGENCY

DRDC Toronto

2. SECURITY CLASSIFICATION

UNCLASSIFIED
Unlimited distribution -

1b. PUBLISHING AGENCY

DRDC Toronto

3. TITLE

(U) MEMS-based light valves for ultra-high resolution projection displays

4. AUTHORS

F. Picard, C. Campillo, K.K. Niall, C. Larouche, H. Jerominek

5. DATE OF PUBLICATION

December 1 , 2002

6. NO. OF PAGES

29

7. DESCRIPTIVE NOTES

8. SPONSORING/MONITORING/CONTRACTING/TASKING AGENCY

Sponsoring Agency:

Monitoring Agency:

Contracting Agency :

Tasking Agency:

9. ORIGINATORS DOCUMENT NO.

Technical Report TR 2002-141

10. CONTRACT GRANT AND/OR
PROJECT NO.

W7711-007650

11. OTHER DOCUMENT NOS.

12. DOCUMENT RELEASABILITY

Unlimited distribution

13. DOCUMENT ANNOUNCEMENT

Unlimited announcement

14. ABSTRACT

(U) Ultra-high resolution projectors will improve the visual systems of military flight simulators dramatically. There are changes in aspect angle and aspect rate which fixed-wing fighter pilots can discriminate at long standoff distances, but which cannot be displayed with adequate resolution by the visual systems of contemporary flight simulators. At present the limit of display resolution is fixed by the capacity of the display's projector. This issue is being addressed by INO, DRDC, and their partners working toward the development of a new light-modulating micromirror MEMS (MicroElectroMechanical Systems). This unique device incorporates $25\text{ }\mu\text{m} \times 25\text{ }\mu\text{m}$ microbridges acting as flexible micromirrors. Each micromirror corresponds to one pixel of an image and is capable of modulating light intensity in analog fashion, with switching speeds in the range of $5\text{ }\mu\text{s}$. A linear array of micromirrors is combined with a scanning system, a microlaser light source and a Schlieren-type optical system to produce a 256 grey-level image. The result is a MOEMS (MicroOptoElectroMechanical Systems)-based system that can write thousands of image lines at a frame rate of 60 Hz.

Finite-element analyses have been performed to describe mechanical properties of the micromirrors. Several examples will be given from both static and dynamic electromechanical simulation. The micromirror fabrication process will be summarized. The physical characteristics of the micromirrors will be reported, including their response time and damage threshold. Finally, future plans including the development of 2000×1 linear pixel arrays with the associated control electronics, will be described.

(U) Les projecteurs à résolution ultra élevée permettront d'améliorer considérablement les systèmes visuels des simulateurs de vol militaires. Des changements sont observés dans la précision de l'angle de présentation et de changement dans cet angle de présentation pouvant être déterminée par les pilotes d'avions à de grandes distances, mais ceux-ci ne peuvent être affichés avec une résolution adéquate par les systèmes de visualisation des simulateurs de vol actuels. À l'heure actuelle, la limite de la résolution d'affichage est fixée par la capacité du projecteur d'affichage. La question est étudiée par l'INO et ses partenaires qui travaillent à l'élaboration d'un nouveau micromiroir MEMS à modulation de lumière (systèmes microélectromécaniques). Ce dispositif unique comprend des microponts de $25\text{ }\mu\text{m} \times 25\text{ }\mu\text{m}$ qui agissent comme des micromiroirs souples. Chaque micromiroir correspond à un pixel d'une image et permet de moduler l'intensité lumineuse de manière analogique, avec des vitesses de commutation de l'ordre de $5\text{ }\mu\text{s}$. Un réseau linéaire de micromiroirs est conjugué à un système de balayage, une source lumineuse à microlaser et à un système optique de type Schlieren en vue de produire une image à 256 niveaux de gris. Le résultat est un système basé sur des systèmes MOEMS (microoptoélectromécaniques) qui permet de tracer des centaines de lignes-images à une fréquence d'images de 60 Hz.

Des analyses par éléments finis ont été réalisées dans le but de décrire les propriétés mécaniques des micromiroirs. Plusieurs exemples seront tirés de la simulation électromécanique statique et dynamique. Le processus de fabrication des micromiroirs sera résumé. Les caractéristiques physiques des micromiroirs seront signalées, incluant leur temps de réponse et le seuil des dommages. Enfin, on décrira les plans à venir, incluant l'élaboration de réseaux de pixels linéaires 2000×1 avec l'électronique de commande connexe.

15. KEYWORDS, DESCRIPTORS or IDENTIFIERS

(U) Microelectromechanical systems; MEMS systems; light modulation; light valve; visual displays; flight simulation; high resolution

Defence R&D Canada

Canada's leader in defence
and national security R&D

R & D pour la défense Canada

Chef de file au Canada en R & D
pour la défense et la sécurité nationale



www.drdc-rddc.gc.ca

